JOC Article
pubs.acs.org/joc

Star-Shaped Donor-π-Acceptor Conjugated Molecules: Synthesis, Properties, and Modification of Their Absorptions Features

Zheng-Ming Tang, Ting Lei, Jin-Liang Wang, Yuguo Ma,* and Jian Pei*

Beijing National Laboratory for Molecular Sciences, the Key Laboratories of Bioorganic Chemistry and Molecular Engineering and of Polymer Chemistry and Physics of Ministry of Education, College of Chemistry and Molecular Engineering, Peking University, Beijing 100871, China

jianpei@pku.edu.cn

Received March 6, 2010

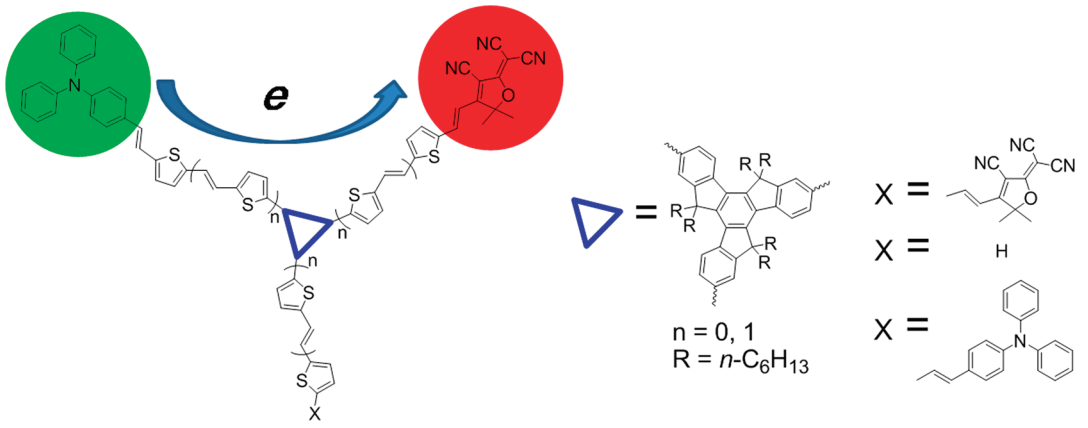

Well-defined star-shaped donor-π-acceptor *meta*-conjugated systems with broad absorption features were constructed through facilely synthetic routes, in which triphenylamine (**TPA**) moiety as an electron donor and 2-dicyanomethylen-3-cyano-4,5,5-trimethyl-2,5-dihydrofuran (**TCF**) unit as an electron acceptor were introduced in various ratios. The investigation of the photophysical properties indicated that the absorption bands of these compounds covered the whole visible range from 300 to 800 nm. For instance, the absorption onset of **D1A2T2** was located at about 780 nm and peaked at 606 nm in thin film. The steady and transient emission spectra showed that these compounds possess an intramolecular energy transfer in such a *meta*-conjugation system, which was further supported by our computational investigation. Our systematic structural variation provides us insight into the tuning strategy of optical properties in D-π-A systems and offered us a series of broad absorption molecules.

Introduction

Donor-π-acceptor conjugated systems have attracted considerable attention due to their unique properties as active materials for organic electronics including organic light-emitting diodes (OLEDs),[1−12] photovoltaic cells,[13−18] nonlinear optics,[19−27] fluorescence imaging,[28,29] and memory.[30−32] Recently, substantial progress has been achieved toward

(1) Thomas, K. R. J.; Huang, T.-H.; Lin, J. T.; Pu, S.-C.; Cheng, Y.-M.; Hsieh, C.-C.; Tai, C. P. *Chem.—Eur. J.* **2008**, *14*, 11231–11241.

(2) (a) Yang, R.; Tian, R.; Hou, Q.; Yang, W.; Cao, Y. *Macromolecules* **2003**, *36*, 7453–7460. (b) Yang, J.; Jiang, C.; Zhang, Y.; Yang, R.; Yang, W.; Hou, Q.; Cao, Y. *Macromolecules* **2004**, *37*, 1211–1218. (c) Hou, Q.; Zhou, Q.; Zhang, Y.; Yang, W.; Yang, R.; Cao, Y. *Macromolecules* **2004**, *37*, 6299–6305. (d) Peng, Q.; Peng, J.-B.; Kang, E.-T.; Neoh, K.-G.; Cao, Y. *Macromolecules* **2005**, *38*, 7292–7298. (e) Peng, Q.; Lu, Z.-Y.; Huang, Y.; Xie, M.-G.; Han, S.-H.; Peng, J.-B.; Cao, Y. *Macromolecules* **2004**, *37*, 260–266.

(3) (a) Wang, J.-L.; Zhou, Y.; Li, Y.; Pei, J. *J. Org. Chem.* **2009**, *74*, 7449–7456. (b) Yang, Y.; Zhou, Y.; He, Q.; He, C.; Yang, C.; Bai, F.; Li, Y. *J. Phys. Chem. B* **2009**, *113*, 7745–7752.

(4) (a) Qian, G.; Dai, B.; Luo, M.; Yu, D.; Zhan, J.; Zhang, Z.; Ma, D.; Wang, Z. Y. *Chem. Mater.* **2008**, *20*, 6208–6216. (b) Qian, G.; Zhong, Z.; Luo, M.; Yu, D.; Zhang, Z.; Ma, D.; Wang, Z. Y. *J. Phys. Chem. C* **2009**, *113*, 1589–1595.

(5) Liu, Y.; Tao, X.; Wang, F.; Dang, X.; Zou, D.; Ren, Y.; Jiang, M. *J. Phys. Chem. C* **2008**, *112*, 3975–3981.

(6) Liu, M. S.; Niu, Y.-H.; Ka, J.-W.; Yip, H.-L.; Huang, F.; Luo, J.; Kim, T.-D.; Jen, A. K.-Y. *Macromolecules* **2008**, *41*, 9570–9580.

Published on Web 04/30/2010 DOI: 10.1021/jo100388c

understanding the structure−property relationships of such conjugated systems.[14a,21,33,34] Their effective charge push−pull effect depends not only on the donor (D) and acceptor (A) groups but also on the effective π-conjugation system and length between donor and acceptor groups. Photon-induced electron transfer (PET) has been largely investigated in these systems because it is a very important process in photovoltaic applications.[35−46]

Although a large number of D-bridge-A (DBA) systems with *para*- and *ortho*-conjugated systems have been investigated, *meta*-conjugated DBA systems are less developed.[47] Both theoretical and experimental studies show that although *meta*-conjugation blocks the delocalization in the ground state, it shows a strong coupling effect in the excited state. Most recently, the investigation of the charge separation and recombination of *meta*-conjugated phenylacetylene demonstrated that *meta*-conjugation style obviously enhanced the charge separation compared with the *para*-conjugation counterparts.[47]

In our previous contributions, we developed a C_3 symmetric and readily modifiable truxene skeleton for OLEDs, organic field-effect transistors (OFETs), and light-harvesting systems.[48] The 2,7,12-trisubstituted truxene unit, as a good *meta*-conjugated system,[49] is similar to the *meta*-conjugated phenyl system investigated by Martinez et al.[47] We modified the truxene unit in the following aspects to investigate

(7) Swanson, S. A.; Wallraff, G. M.; Chen, J. P.; Zhang, W.; Bozano, L. D.; Carter, K. R.; Salem, J. R.; Villa, R.; Scott, J. C. *Chem. Mater.* **2003**, *15*, 2305–2312.
(8) Jin, S.-H.; Kim, M.-Y.; Koo, D.-S.; Kim, Y.-I.; Park, S.-H.; Lee, K.; Gal, Y.-S. *Chem. Mater.* **2004**, *16*, 3299–3307.
(9) Chen, C.-T. *Chem. Mater.* **2004**, *16*, 4389–4400.
(10) Zhu, Y.; Kulkarni, A. P.; Jenekhe, S. A. *Chem. Mater.* **2005**, *17*, 5225–5257.
(11) Chen, A. C.-A.; Wallace, J. U.; Klubek, K. P.; Madaras, M. B.; Tang, C. W.; Chen, S. H. *Chem. Mater.* **2007**, *19*, 4043–4048.
(12) Leung, M.-K.; Chang, C.-C.; Wu, M.-H.; Chuang, K.-H.; Lee, J.-H.; Shieh, S.-J.; Lin, S.-C.; Chiu, C.-F. *Org. Lett.* **2006**, *8*, 2623–2626.
(13) (a) Peet, J.; Kim, J. Y.; Coates, N. E.; Ma, W. L.; Moses, D.; Heeger, A. J.; Bazan, G. C. *Nat. Mater.* **2007**, *6*, 497–500. (b) Kim, J. Y.; Lee, K.; Coates, N. E.; Moses, D.; Nguyen, T.-Q.; Dante, T.-M.; Heeger, A. J. *Science* **2007**, *317*, 222–225.
(14) (a) Cravino, A.; Leriche, P.; Alévêque, O.; Roquet, S.; Roncali, J. *Adv. Mater.* **2006**, *18*, 3033–3037. (b) Roquet, S.; Cravino, A.; Leriche, P.; Alévêque, O.; Frère, P.; Roncali, J. *J. Am. Chem. Soc.* **2006**, *128*, 3459–3466. (c) Bettignies, R. D.; Nicolas, Y.; Blanchard, P.; Levillain, E.; Nunzi, J.-M.; Roncali, J. *Adv. Mater.* **2003**, *15*, 1939–1943.
(15) Lai, M.-H.; Chueh, C.-C.; Chen, W.-C.; Wu, J.-L.; Chen, F.-C. *J. Polym. Sci., Part A: Polym. Chem.* **2008**, 973–985.
(16) Xia, P. F.; Feng, X. J.; Lu, J.; Tsang, S.-W.; Movileanu, R.; Tao, Y.; Wong, M. S. *Adv. Mater.* **2008**, *20*, 4810–4815.
(17) (a) Chen, J.; Cao, Y. *Acc. Chem. Res.* **2009**, *42*, 1709–1718. (b) Yang, R.; Tian, R.; Yan, J.; Zhang, Y.; Yang, J.; Hou, Q.; Yang, W.; Zhang, C.; Cao, Y. *Macromolecules* **2005**, *38*, 244–253. (c) Wang, E.; Wang, M.; Wang, L.; Duan, C.; Zhang, J.; Cai, W.; He, C.; Wu, H.; Cao, Y. *Macromolecules* **2009**, *42*, 4410–4415.
(18) (a) Zhan, X.; Tan, Z.; Domercq, B.; An, Z.; Zhang, X.; Barlow, S.; Li, Y.; Zhu, D.; Kippelen, B.; Marder, S. R. *J. Am. Chem. Soc.* **2007**, *129*, 7246–7247. (b) He, C.; He, Q.; Yang, X.; Wu, G.; Yang, C.; Bai, F.; Shuai, Z.; Wang, L.; Li, Y. *J. Phys. Chem. C* **2007**, *111*, 8661–8666. (c) Zhao, G.; Wu, G.; He, C.; Bai, F.-Q.; Xi, H.; Zhang, H.-X.; Li, Y. *J. Phys. Chem. C* **2009**, *113*, 2636–2642. (d) Zhang, J.; Yang, Y.; He, C.; He, Y.; Zhao, G.; Li, Y. *Macromolecules* **2009**, *42*, 7619–7622.
(19) (a) Ohira, S.; Rudra, I.; Schmidt, K.; Barlow, S.; Chung, S.-J.; Zhang, Q.; Matichak, J.; Marder, S. R.; Brédas, J.-L. *Chem.—Eur. J.* **2008**, *14*, 11082–11091. (b) Albota, M.; Beljonne, D.; Brédas, J.-L.; Ehrlich, J.-E.; Fu, J.-Y.; Heikal, A. A.; Hess, S. E.; Kogej, T.; Levin, M. D.; Marder, S. R.; McCord-Maughon, D.; Perry, J. W.; Röckel, H.; Rumi, M.; Subramaniam, G.; Webb, W. W.; Wu, X.-L.; Xu, C. *Science* **1998**, *281*, 1653–1656. (c) Chung, S. J.; Rumi, M.; Alain, V.; Barlow, S.; Perry, J. W.; Marder, S. R. *J. Am. Chem. Soc.* **2005**, *127*, 10844–10845. (d) Pond, S. J. K.; M. Rumi, M.; M. D. Levin, M. D.; T. C. Parker, T. C.; D. Beljonne, D. M. W. Day, M. W.; Brédas, J.-L.; Marder, S. R.; Perry, J. W. *J. Phys. Chem. A* **2002**, *106*, 11470–11480. (e) Meyers, F.; Chen, C. T.; Marder, S. R.; Brédas, J.-L. *Chem.—Eur. J.* **1997**, *3*, 530–537. (f) Davies, J. A.; Elangovan, A.; Sullivan, P. A.; Olbricht, B. C.; Bale, D. H.; Ewy, T. R.; Isborn, C. M.; Eichinger, B. E.; Robinson, B. H.; Reid, P. J.; Li, X.; Dalton, L. R. *J. Am. Chem. Soc.* **2008**, *130*, 10565–10575. (g) Pond, S. J. K.; Tsutsumi, O.; Rumi, M.; Kwon, O.; Zojer, E.; Brédas, J.-L.; Marder, S. R.; Perry, J. W. *J. Am. Chem. Soc.* **2004**, *126*, 9291–9306.(h) Collings, J. C.; Poon, S.-Y.; Droumaguet, C. L.; Charlot, M.; Katan, C.; Palsson, L.-O.; Beeby, A.; Mosely, J. A.; Kaiser, H. M.; Kaufmann, D.; Wong, W.-Y.; Blanchard-Desce, M.; Marder, T. B. *Chem.—Eur. J.* **2009**, *15*, 198–208. (i) Beverina, L.; Fu, J.; Leclercq, A.; Zojer, E.; Pacher, P.; Barlow, S.; Stryland, E. W. V.; Hagan, D. J.; Brédas, J.-L.; Marder, S. R. *J. Am. Chem. Soc.* **2005**, *127*, 7282–7283.
(20) Lee, H. J.; Sohn, J.; Hwang, J.; Park, S. Y.; Choi, H.; Cha, M. *Chem. Mater.* **2004**, *16*, 456–465.
(21) Abbotto, A.; Beverina, L.; Bozio, R.; Facchetti, A.; Ferrante, C.; Pagani, G. A.; Pedron, D.; Signorini, R. *Org. Lett.* **2002**, *4*, 1495–1498.
(22) (a) Maciel, G. S.; Kim, K.-S.; Chung, S.-J.; Swiatkiewicz, J.; He, G. S.; Prasad, P. N. *J. Phys. Chem. B* **2001**, *105*, 3155–3157. (b) Brousmiche, D. W.; Serin, J. M.; Fréchet, J. M. J.; He, G. S.; Lin, T.-C.; Chung, S.-J.; Prasad, P. N. *J. Phys. Chem. B* **2004**, *108*, 8592–8600. (c) Kannan, R.; He, G. S.; Lin, T.-C.; Prasad, P. N. *Chem. Mater.* **2004**, *16*, 185–194.
(23) Yang, W. J.; Kim, D. Y.; Jeong, M.-Y.; Kim, H. M.; Lee, Y. K.; Fang, X.; Jeon, S.-J.; Cho, B. R. *Chem.—Eur. J.* **2005**, *11*, 4191–4198.
(24) Kay, A. J.; Woolhouse, A. D.; Zhao, Y.; Clays, K. *J. Mater. Chem.* **2004**, *14*, 1321–1330.
(25) (a) He, M.; Leslie, T. M.; Sinicropi, J. A. *Chem. Mater.* **2002**, *14*, 4662–4668. (b) He, M.; Leslie, T.; Garner, S.; DeRosa, M.; Cites, J. *J. Phys. Chem. B* **2004**, *108*, 8731–8736.
(26) (a) Liao, Y.; Eichinger, B. E.; Firestone, K. A.; Haller, M.; Luo, J.; Kaminsky, W.; Benedict, J. B.; Reid, P. J.; Jen, A. K.-Y.; Dalton, L. R.; Robinson, B. H. *J. Am. Chem. Soc.* **2005**, *127*, 2758–2766. (b) Liao, Y.; Bhattacharjee, S.; Firestone, K. A.; Eichinger, B. E.; Paranji, R.; Anderson, C. A.; Robinson, B. H.; Reid, P. J.; Dalton, L. R. *J. Am. Chem. Soc.* **2006**, *128*, 6847–6853. (c) Kim, T.-D.; Kang, J.-W.; Luo, J.; Jang, S.-H.; Ka, J.-W.; Tucker, N.; Benedict, J. B.; Dalton, L. R.; Gray, T.; Overney, R. M.; Park, D. H.; Herman, W. N.; Jen, A. K.-Y. *J. Am. Chem. Soc.* **2007**, *129*, 488–489. (d) Sullivan, P. A.; Rommel, H.; Liao, Y.; Olbricht, B. C.; Akelaitis, A. J. P.; Firestone, K. A.; Kang, J.-W.; Luo, J.; Davies, J. A.; Choi, D. H.; Eichinger, B. E.; Reid, P. J.; Chen, A.; Jen, A. K.-Y.; Robinson, B. H.; Dalton, L. R. *J. Am. Chem. Soc.* **2007**, *129*, 7523–7530. (e) Luo, J.; Cheng, Y.-J.; Kim, T.-D.; Hau, S.; Jang, S.-H.; Shi, Z.; Zhou, X.-H.; Jen, A. K.-Y. *Org. Lett.* **2006**, *8*, 1387–1390.
(27) He, G. S.; Tan, L. S.; Zheng, Q.; Prasad, P. N. *Chem. Rev.* **2008**, *108*, 1245–1330.
(28) Bouffard, J.; Kim, Y.; Swager, T. M.; Weissleder, R.; Hilderbrand, S. A. *Org. Lett.* **2008**, *10*, 37–40.
(29) Lord, S. J.; Conley, N. R.; Lee, H. L. D.; Samuel, R.; Liu, N.; Twieg, R. J.; Moerner, W. E. *J. Am. Chem. Soc.* **2008**, *130*, 9204–9205.
(30) Nishimura, S. Y.; Lord, S. J.; Klein, L. O.; Willets, K. A.; He, M.; Lu, Z.; Twieg, R. J.; Moerner, W. E. *J. Phys. Chem. B* **2006**, *110*, 8151–8157.
(31) Ling, Q.-D.; Song, Y.; Lim, S.-L.; Teo, E. Y-H; Tan, Y.-P.; Zhu, C.; Chan, D. S. H.; Kwong, D-L; Kang, E.-T.; Neoh, K.-G. *Angew. Chem., Int. Ed.* **2006**, *45*, 2947–2951.
(32) (a) Shang, Y.; Wen, Y.; Li, S.; Du, S.; He, X.; Cai, L.; Li, Y.; Yang, L.; Gao, H.; Song, Y. *J. Am. Chem. Soc.* **2007**, *129*, 11674–11675. (b) Jiang, G.; Song, Y.; Guo, X.; Zhang, D.; Zhu, D. *Adv. Mater.* **2008**, *20*, 2888–2898.
(33) Meier, H. *Angew. Chem., Int. Ed.* **2005**, *44*, 2482–2506.
(34) Sapsford, K. E.; Berti, L.; Medintz, I. L. *Angew. Chem., Int. Ed.* **2006**, *45*, 4562–4588.
(35) Zhao, G.-J.; Chen, R.-K.; Sun, M.-T.; Liu, J.-Y.; Li, G.-Y.; Gao, Y.-L.; Han, K.-L.; Yang, X.-C.; Sun, L. *Chem.—Eur. J.* **2008**, *14*, 6935–6947.
(36) Kosower, E. M. *Acc. Chem. Res.* **1982**, *15*, 259–266.
(37) Michael, N. P.-R. *Acc. Chem. Res.* **1994**, *27*, 18–25.
(38) Masuhara, H.; Mataga, N. *Acc. Chem. Res.* **1981**, *14*, 312–318.
(39) Rosokha, S. V.; Kochi, J. K. *Acc. Chem. Res.* **2008**, *41*, 641–653.
(40) Brouwer, A. M.; Eijckelhoff, C.; Willemse, R. J.; Verhoeven, J. W.; Schuddeboom, W.; Warman, J. M. *J. Am. Chem. Soc.* **1993**, *115*, 2988–2989.
(41) Ramos, A. M.; Meskers, S. C. J.; Beckers, E. H. A.; Prince, R. B.; Brunsveld, L.; Janssen, R. A. J. *J. Am. Chem. Soc.* **2004**, *126*, 9630–9644.
(42) Yonemoto, E. H.; Kim, Y.; Schmehl, R. H.; Wallin, J. O.; Shoulders, B. A.; Richardson, B. R.; Haw, J. F.; Mallouk, T. E. *J. Am. Chem. Soc.* **1994**, *116*, 10557–10563.
(43) Roberts, J. A.; Kirby, J. P.; Nocera, D. G. *J. Am. Chem. Soc.* **1995**, *117*, 8051–8052.
(44) Dijk, S. I. V.; Groen, C. P.; Hartl, F.; Brouwer, A. M.; Verhoeven, J. W. *J. Am. Chem. Soc.* **1996**, *118*, 8425–8432.
(45) Heitele, H.; Michel-Beyerle, M. E. *J. Am. Chem. Soc.* **1985**, *107*, 8286–8288.
(46) Wasielewski, M. R.; Niemczyk, M. P. *J. Am. Chem. Soc.* **1984**, *106*, 5043–5045.
(47) (a) Thompson, A. L.; Ahn, T.-S.; Thomas, K. R. J.; Thayumanavan, S.; Martínez, T. J.; Bardeen, C. J. *J. Am. Chem. Soc.* **2005**, *127*, 16348–16349. (b) Kevin M. Gaab, K. M.; Thompson, A. L.; Xu, J.; Martínez, T. J.; Bardeen, C. J. *J. Am. Chem. Soc.* **2003**, *125*, 9288–9289.

CHART 1. Molecular Structures of D1A1T1, D2A1T1, D1A2T1, D1A1T2, D2A1T2, and D1A2T2

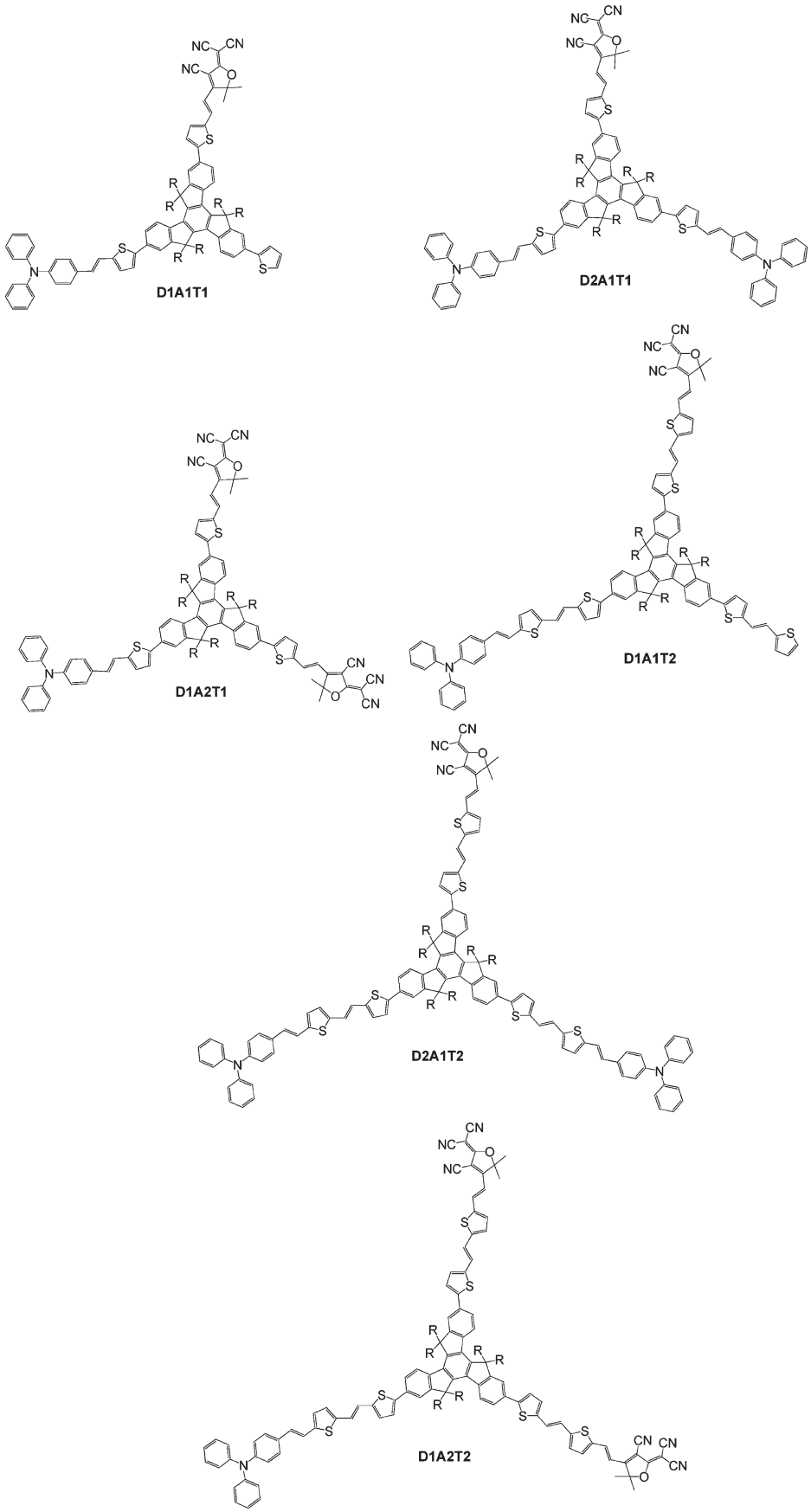

SCHEME 1. Synthetic Approach to D-π-A Truxene-Linker Chromophores D1A1T2, D1A2T2, and D2A1T2

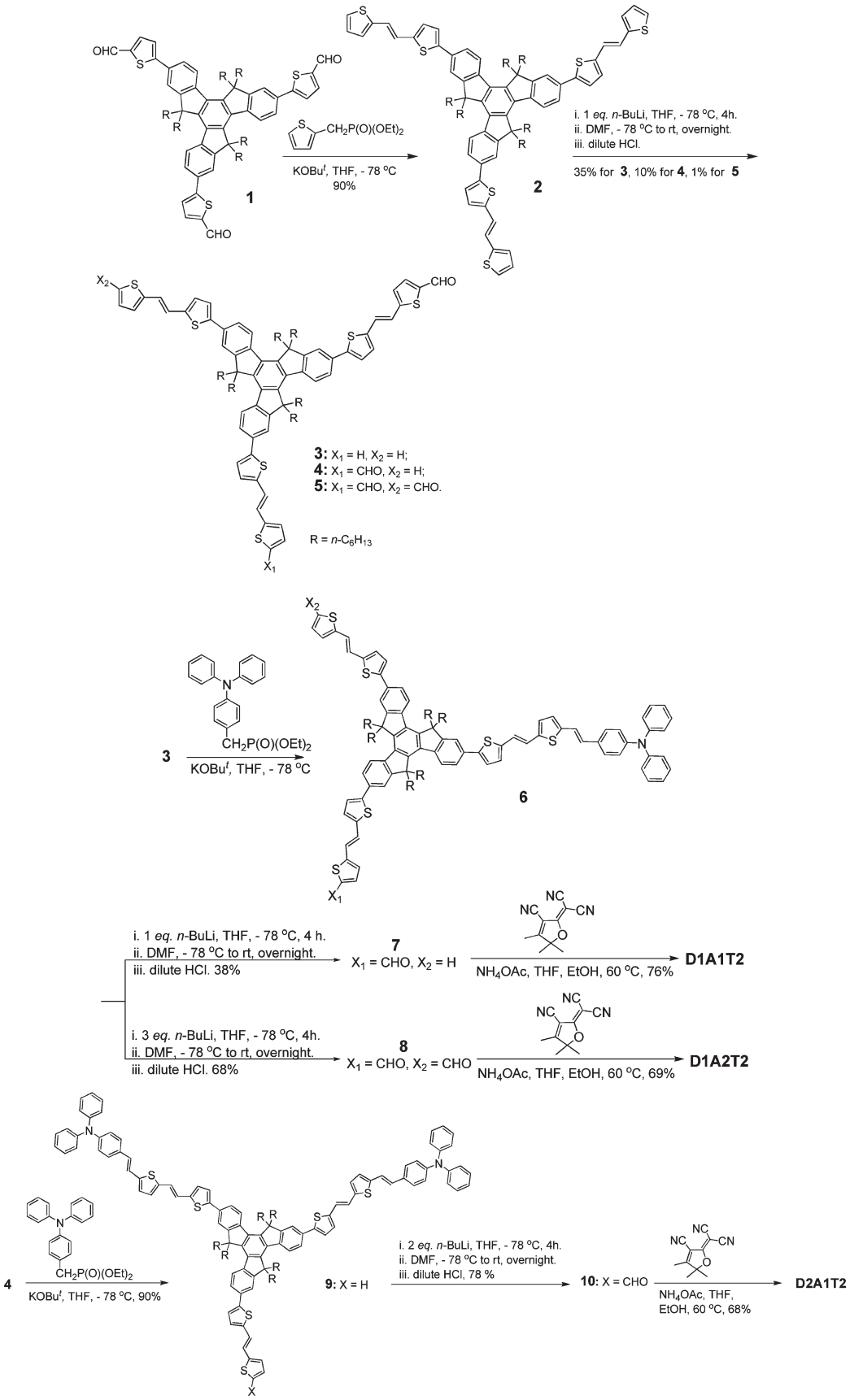

SCHEME 2. Synthetic Approach to D-π-A Truxene-Linker Chromophores D1A2T1, D1A1T1, and D2A1T1

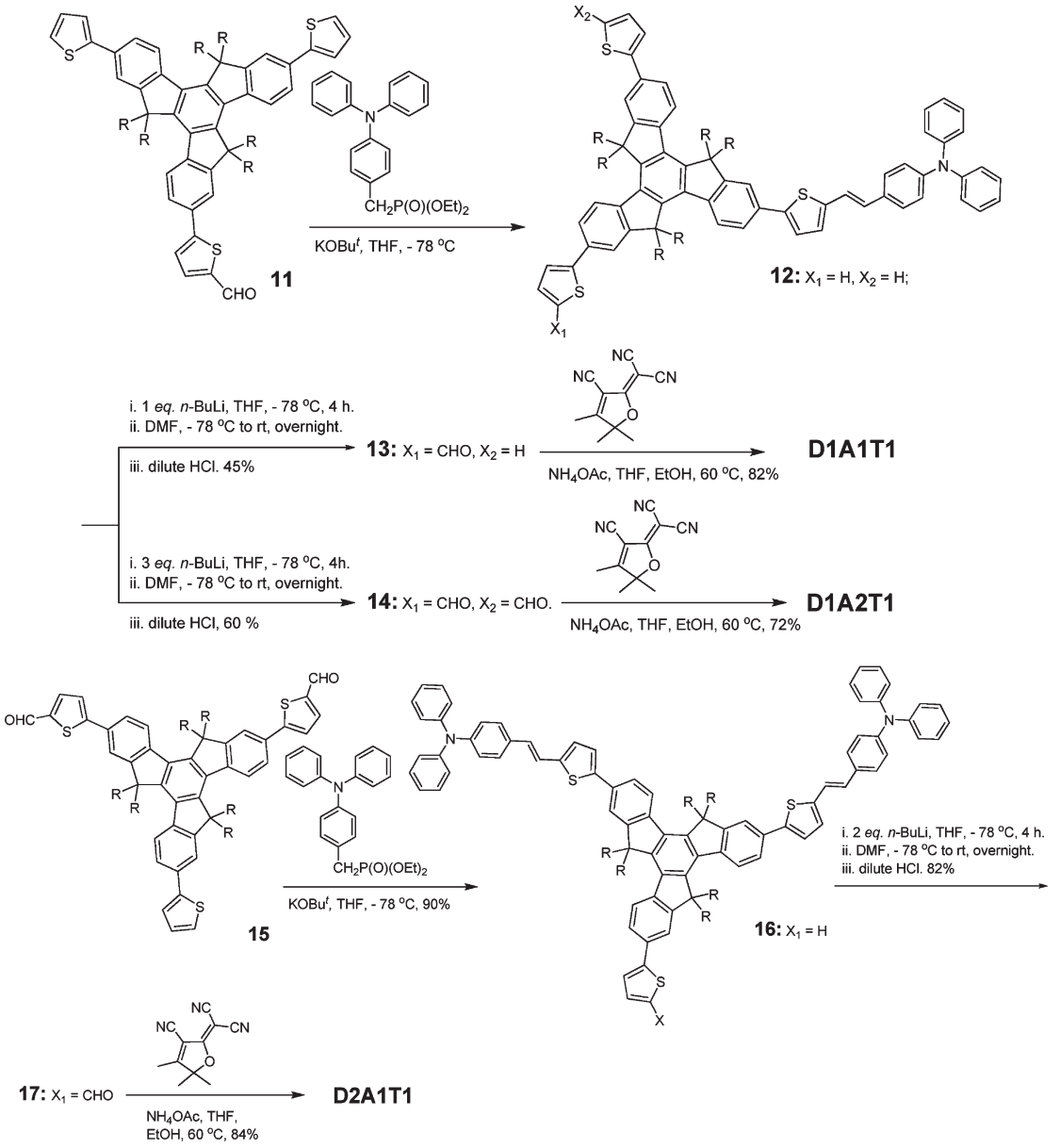

meta-conjugated DBA systems: (1) tuning the D−A ratios and (2) introducing different linkers between the donor and acceptors. Herein, we present the synthesis, characterization, photophysical and electrochemical properties and theoretical investigation of star-shaped D-π-A chromophores with arms of varying length, **D1A1T1**, **D2A1T1**, **D1A2T1**, **D1A1T2**, **D2A1T2**, and **D1A2T2**, in which a triphenylamine (**TPA**) unit is employed as an electron donor and 2-dicyanomethylen-3-cyano-4,5,5-trimethyl-2,5-dihydrofuran (**TCF**) moiety as an electron acceptor. Their molecular structures are shown in Chart 1. The systematic structural variation provides us insight into the tuning strategy of optical properties in D-π-A systems and offered us a series of broad absorption molecules.

Results and Discussion

Synthesis. Scheme 1 illustrates the synthetic approach to these D-π-A truxene-linker chromophores, **D1A1T1**, **D2A1T1**, **D1A2T1**, **D1A1T2**, **D2A1T2**, and **D1A2T2**. The Horner−Emmons coupling reaction between compound **1**[48d] and diethyl thiophen-2-ylmethylene phosphonate[50] afforded **2** in 90% yield. Treatment of **2** with *n*-butyllithium followed by adding DMF at −78 °C and then hydrolyzing gave a mixture of aldehydes **3**, **4**, and **5** in moderate yield, which

(48) (a) Pei, J.; Wang, J.-L.; Cao, X.-Y.; Zhou, X.-H.; Zhang, W.-B. *J. Am. Chem. Soc.* **2003**, *125*, 9944–9945. (b) Cao, X.-Y.; Liu, X.-H.; Zhou, X.-H.; Zhang, Y.; Jiang, Y.; Cao, Y.; Cui, Y.-X.; Pei, J. *J. Org. Chem.* **2004**, *69*, 6050–6058. (c) Cao, X.-Y.; Zhang, W.-B.; Wang, J.-L.; Zhou, X.-H.; Lu, H.; Pei, J. *J. Am. Chem. Soc.* **2003**, *125*, 12430–12431. (d) Wang, J.-L.; Duan, X.-F.; Jiang, B; Gan, L.-B.; Pei, J.; He, C.; Li, Y. *J. Org. Chem.* **2006**, *71*, 4400–4410. (e) Wang, J.-L.; Tang, Z.-M.; Xiao, Q.; Ma, Y.; Pei, J. *Org. Lett.* **2008**, *10*, 4271–4274.

(49) Yang, J.-S.; Huang, H.-H.; Ho, J.-H. *J. Phys. Chem. B* **2008**, *112*, 8871–8878.

(50) Hou, J.; Tan, Z.; Yan, Y.; He, Y.; Yang, C.; Li, Y. *J. Am. Chem. Soc.* **2006**, *128*, 4911–4916.

SCHEME 3. Molecular Structures of Model Compounds D3T1, A3T1, D3T2, and A3T2

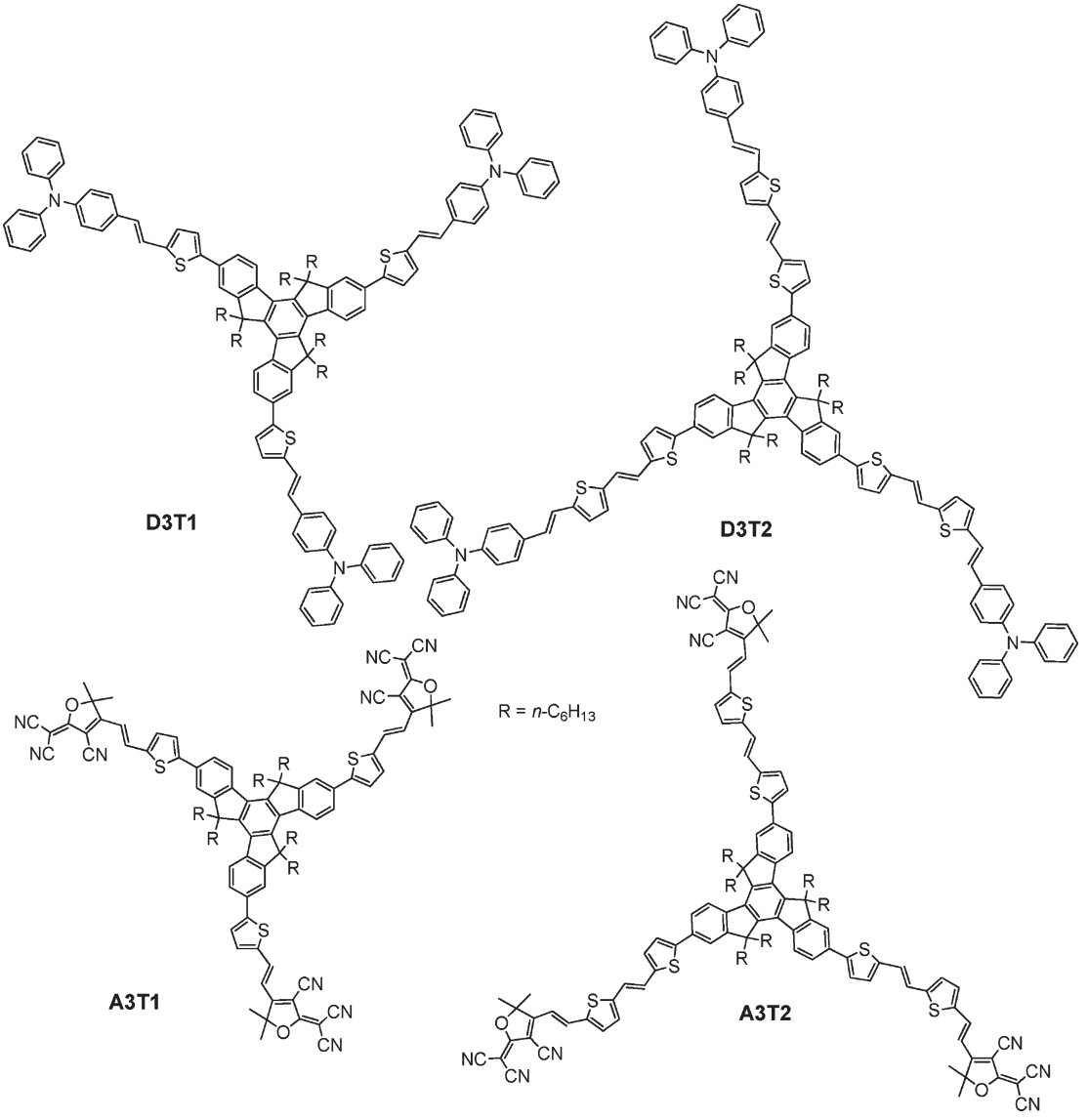

were easily separated and purified via flash chromatography. The Horner−Emmons coupling reaction between monoaldehyde **3** and 4-(diphenylamino)benzyl phosphonate yielded **6**. The reaction of **6** with various equivalents of *n*-BuLi followed by adding DMF at −78 °C to give **7** or **8**, respectively. We employed the typical Knoevenagel reaction condition for the condensation of **TCF** and **8** to give compound **D1A2T2** in poor yield.[26] After we adapted NH_4OAc as a base in a solvent mixture of THF and EtOH at 60 °C for 4 h, the yield of this condensation for **D1A2T2** was increased to 76%. **D1A1T2** was also obtained through the condensation of **TCF** and **7** at the same condition in 69% yield. As shown in Schemes 1 and 2, following the same procedures, other D-π-A star-shaped chromophores **D2A1T2**, **D1A1T1**, **D2A1T1**, and **D1A2T1** were obtained in good yields.

For the comparison, we also prepared the corresponding model compounds **D3T1**, **A3T1**, **D3T2**, and **A3T2** as shown in Scheme 3 (see Supporting Information). All compounds were readily soluble in common organic solvents, such as toluene, THF, and CH_2Cl_2. The structures and purity of all new compounds were fully characterized and verified by ^1H and ^{13}C NMR, elemental analysis, and MALDI-TOF MS.

Computational Modeling Studies. To visualize geometries and electronic structures of these six compounds, computational studies were performed before synthesis with density functional theory (DFT) using the B3LYP/6-31G(d)//B3LYP/3-21G* level.[51,52] All hexyl substituents were replaced with methyl groups for simplicity. Figure 1 shows the molecular geometries and the HOMO−LUMO surfaces of **D1A1T1**, **D1A2T1**, and **D2A1T1**. The truxene cores exhibited good planarity, and the thienylenevinylenes showed a banana-shaped configuration. As expected, the HOMOs of these compounds were mostly found on the **TPA** conjugated arms, and in contrast the LUMOs mostly existed on the **TCF** segments. Because of the *meta*-substituted truxene cores, the

(51) Frisch, M. J. et al. *Gaussian 03, Revision C.02*; Gaussian, Inc.: Wallingford, CT, **2004**.

(52) Dennington, R., II; Keith, T.; Millam, J.; Eppinnett, K.; Hovell, W. L.; Gilliland, R. *GaussView, Version 3.09*; Semichem, Inc.: Shawnee Mission, KS, **2003**.

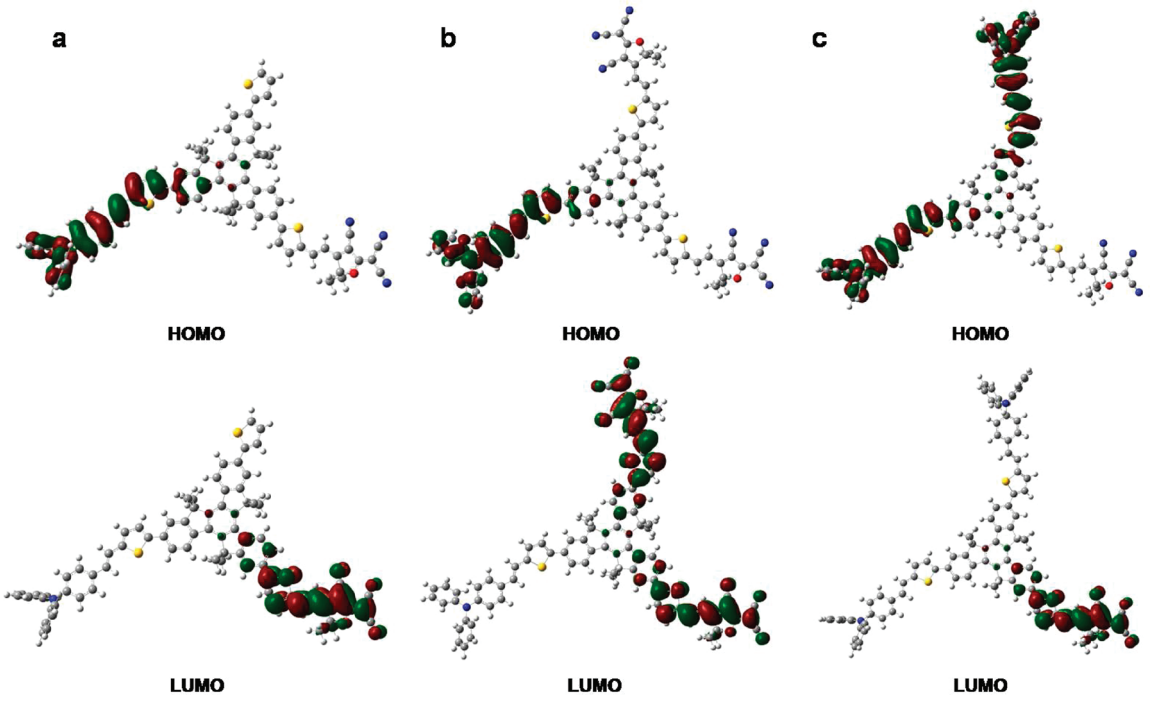

FIGURE 1. B3LYP/6-31G(d)//B3LYP/3-21G* level calculated structures and the HOMO (top) and LUMO (bottom) surfaces of (a) **D1A1T1**, (b) **D1A2T1**, and (c) **D2A1T1**. The LUMO of **D1A2T1** and the HOMO of **D2A1T1**a re composed of two degenerated orbitals.

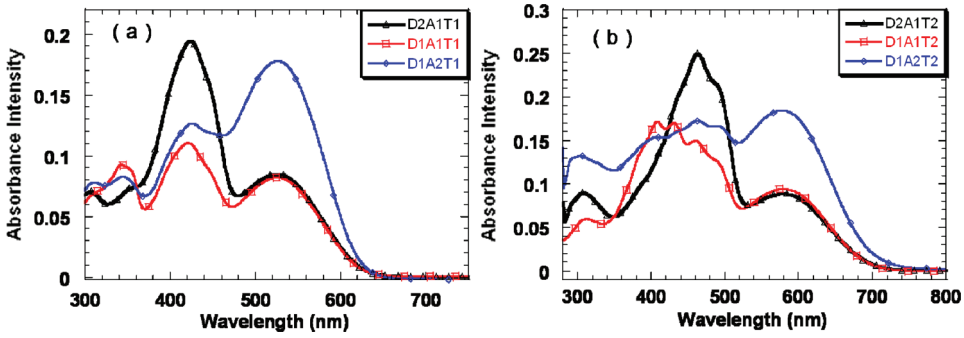

FIGURE 2. Absorption spectra of **D2A1T1**, **D1A1T1**, and **D1A2T1** (a) and of **D2A1T2**, **D1A1T2**, and **D1A2T2** (b) in THF solution (10^{-6} M).

HOMOs and the LUMOs were found to be intercepted at the center; however, the delocalization of the whole molecule still expanded well for other orbitals. For example, HOMO−1, LUMO+1, etc. for **D1A1T1** suggested the appreciable interactions between donors and acceptors (Figure S1 in Supporting Information). The calculated gas-phase HOMO−LUMO gaps were found to be 1.44−1.50 eV for **D1A1T1**, **D1A2T1**, and **D2A1T1** and 1.31−1.33 eV for **D1A1T2**, **D2A1T2**, and **D1A2T2**, respectively (Table 4). The calculated band gaps of the molecules were narrower than the observed molecular absorption band gaps (see Table 4). These results indicated that there are no direct transitions from the HOMO to the LUMO. For **D1A1T1**, the absorption peaks are not the direct transition from the HOMO to the LUMO; the absorption of the TPA part can be attributed to the transition from the HOMO to LUMO+1. Although its HOMO and the LUMO are disjunct, the LUMO+1 and LUMO are partially overlapped (Figure S1 in Supporting Information). Therefore, we prefer that an excited electron transfer might exist in this system.

Photophysical Properties. The absorption and emission spectra of these star-shaped D-π-A compounds were measured in dilute THF solution. Figure 2a shows the comparison of absorption spectra of **D2A1T1**, **D1A1T1**, and **D1A2T1** in dilute THF solution (10^{-6} M). For **D1A1T1**, in which the ratio of **TPA** (donor) and **TCF** (acceptor) groups is 1, it was observed the maximum absorption peak λ_{max} at about 424 nm with other two absorption bands at about 321 and 526 nm. Compared with model compounds **D3T1** and **A3T1**, these three absorption bands were coarsely assigned to three different absorption fragments: the thiophene-functionalized truxene core (321 nm), thienylvinylene-**TPA** (424 nm), and thienylvinylene-**TCF** units (526 nm), respectively. **D1A2T1**, in which the ratio of **TPA** and **TCF** groups is 1:2, exhibited the similar three absorption bands as **D2A1T1**, in which the ratio of **TPA** and **TCF** groups is 2:1, although these absorption peaks showed various molar extinction coefficients. The absorption features of **D2A1T1**, **D1A1T1**, and **D1A2T1** covered from 300 to 640 nm, almost the whole visible range, which was due to the combination of three absorption bands.

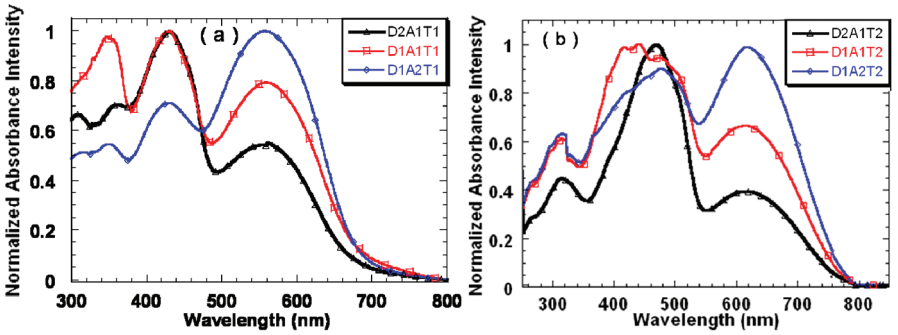

FIGURE 3. Absorption spectra of **D2A1T1**, **D1A1T1**, and **D1A2T1** (a) and of **D2A1T2**, **D1A1T2**, and **D1A2T2** (b) in the solid state.

Figure 2b shows the absorption spectra of **D1A1T2**, **D2A1T2**, and **D1A2T2** in THF solution (10^{-6} M). For **D2A1T2**, in which the ratio of **TPA** and **TCF** groups is 2, its absorption features showed two major peaks at 462 and 578 nm in THF solution (10^{-6} M). The red shift of the absorption band of **D2A1T2** was observed compared to **D2A1T1** (462 nm vs 424 and 578 nm vs 526 nm, respectively), which was due to the increase of the effective conjugation length. **D3T2** showed the absorption maximum λ_{max} at 461 nm in THF solution. Moreover, the absorption maximum λ_{max} for **A3T2** peaked at 580 nm in THF solution (10^{-6} M). The splitting of the absorption bands at about 400 to 490 nm was observed from **D1A1T2** and **D1A2T2**. All the absorption behaviors are in accordance with our theoretical investigation that the *meta*-conjugated arms are not coupled at the ground state.

The absorption of these compounds in thin film as shown in Figure 3 displayed similar features as in solution; however, it was observed that three absorption peaks of **D1A1T1** showed different red shifts: 5 nm for the truxene part, 10 nm for the **TPA** part, and 20 nm for the **TCF** part. Due to strong molecular interactions, its onset moved from 610 nm to about 700 nm. Comparison of the solution and solid-state spectra of **D2A1T2** and **D2A1T1** revealed that the absorption spectra of **D2A1T2** covered much broader range. By contrast with the absorption spectra of **D2A1T2**, **D1A1T2**, and **D1A2T2**, as shown in Figure 3a,b, their absorption features indicated that the increasing of the ratio of **TCF** and **TPA** induced a successive decrease of the absorbance intensity of the donor branch and an obvious increase of the absorbance intensity of the acceptor branch. The photophysical properties of these compounds in solution and in thin film were summarized in Table 1.

Figure 4a shows the photoluminence spectra of **D2A1T1**, **D1A1T1**, and **D1A2T1** in THF solution (10^{-6} M). A successive photoluminescence decrease was observed with more **TCF** introduced into the star-shaped systems. For **D2A1T2**, **D1A1T2**, and **D1A2T2**, similar photoluminescence decrease phenomenon were observed with a red shift of the photoluminescence maximum due to longer conjugation (Figure 4b). The fluorescence quenching of the emission of **TPA** segment, as the increase of the **TCF**, indicated there might exit another exciton quenching pathways, such as photoinduced electron transfer (PET)[53] and energy transfer

TABLE 1. Summary of Photophysical Properties in Solution and in Thin Film

		absorption λ_{max} (nm)		
compound	aborption λ_{onset} in thin film (nm)	in solution[a]	in film	ε_1[b], ε_2[c] ($\times 10^5$ M^{-1} cm^{-1})
D2A1T1	720	526	556	1.95, 0.85
D1A1T1	720	526	555	1.10, 0.82
D1A2T1	720	526	557	1.26, 1.80
D2A1T2	780	578	607	2.50, 0.90
D1A1T2	780	579	607	1.48, 0.95
D1A2T2	780	578	608	1.73, 1.85

[a]Measured in THF solution (10^{-6} M). [b]ε of shorter wave peak. [c]ε of longer wave peak.

(Forster or Dexter).[53,54] In the DBA systems, the PET and super exchange mechanism (modification of Dexter theory) are preferred.[55] As investigated by Bardeen et al. in the *meta*-conjugated phenylacetylene DBA system, they proposed that the process is a PET mechanism and the *meta*-conjugation system shows a longer time of electron separation state.[47a]

To investigate the solvent effect on photophysical behaviors of these D-π-A compounds, we also measured their photophysical spectra in different solvents varying from cyclohexane to DMSO in sequence of dielectric constants. In contrast with *para*-conjugated compounds, solvent effects of these *meta*-conjugated compounds are not so dramatic, indicating that the electronic interactions in the ground state are weak.[19f] The absorption bands of the donor branches in these D-π-A compounds did not exhibit obvious shift; however, the acceptor branch absorption varied relatively obviously in these solvents. In low polar solvents, the absorption maximum λ_{max} of the acceptor branch showed an obvious red shift upon increasing the solvent dielectric constant; for example, the absorption maximum λ_{max} of **D2A1T1** peaked at 519 nm in cyclohexane and at 527 nm in toluene; in more highly polar solvents, the increase of dielectric constant of solvents, it also induced obvious red shift and moved to 532 nm in DMF and 537 nm in DMSO (Figure S5 in Supporting Information, Table 2). The similar results were also observed from other five D-π-A molecules (Table 2). DCM seems to be a special solvent for such kind of systems, which might be due to special interaction between these molecules and DCM.

However, photoluminescent spectra of these compounds exhibited distinct solvent dependence. Figure 5 shows the emission spectra of **D2A1T1** in cyclohexane and DMSO

(53) Holman, M. W.; Liu, R.; Zang, L.; Yan, P.; DiBenedetto, S. A.; Bowers, R. D.; Adams, D. M. *J. Am. Chem. Soc.* **2004**, *126*, 16126–16133.
(54) Osuka, A.; Noya, G.; Taniguchi, S.; Okada, T.; Nishimura, Y.; Yamazaki, I.; Mataga, N. *Chem.—Eur. J.* **2000**, *6*, 33–46.
(55) Speiser, S. *Chem. Rev.* **1996**, *96*, 1953–1976.

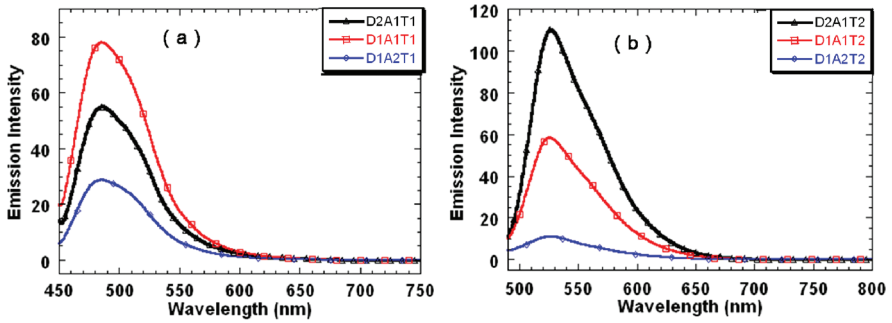

FIGURE 4. Emission spectra of **D2A1T1**, **D1A1T1**, and **D1A2T1** upon excitation at 423 nm (a) and of **D2A1T2**, **D1A1T2**, and **D1A2T2** upon excitation at 460 nm (b) in THF solution (10^{-6} M).

TABLE 2. Summary of Solvent Effect on Photophysical Behaviors of the D-π-A Compounds

	cyclohexane		toluene		DCM		THF		DMF		DMSO	
compound	$\lambda_{max}{}^a$	$\lambda_{em}{}^b$	$\lambda_{max}{}^a$	$\lambda_{em}{}^b$	$\lambda_{max}{}^a$	$\lambda_{em}{}^b$	$\lambda_{max}{}^a$	$\lambda_{em}{}^b$	$\lambda_{max}{}^a$	$\lambda_{em}{}^b$	$\lambda_{max}{}^a$	$\lambda_{em}{}^b$
D2A1T1	422, 519	468, 600	426, 527	458	423, 548	491	423, 526	486	423, 532	502	426, 537	512
D1A1T1	423, 518	468, 601	424, 526	456	424, 548	492	422, 526	486	424, 534	503	426, 538	512
D1A2T1	423, 518	468, 602	424, 527	458	423, 548	491	423, 526	485	424, 534	503	425, 538	512
D2A1T2	460, 572	514	465, 579	522	463, 602	532	462, 578	527	462, 584	545	467, 591	556
D1A1T2	461, 573	513	464, 581	519	460, 601	531	461, 579	526	461, 586	544	466, 592	553
D1A2T2	462, 572	514	465, 580	521	462, 602	532	463, 578	526	462, 586	543	467, 593	554

^{a}Absorption peaks in nm (10^{-6} M). ^{b}Emission peaks in nm. Measured in solutions (10^{-6} M).

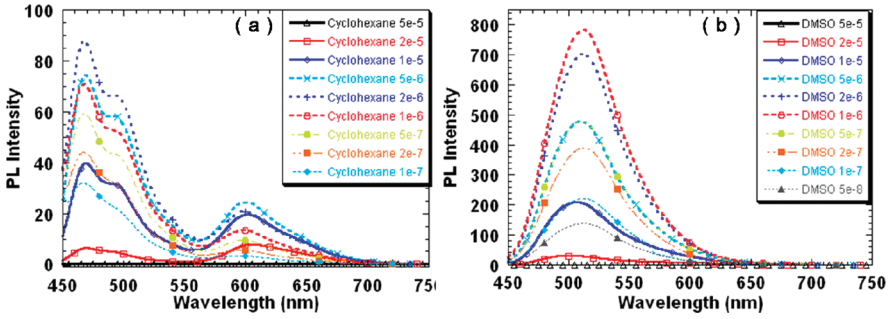

FIGURE 5. PL spectra of **D2A1T1** in cyclohexane (a) and in DMSO (b). Emission spectra were obtained upon excitation at 423 nm.

upon excitation at 423 nm, respectively (10^{-6} M). In cyclohexane, an obvious peak in longer wavelength region appeared, which can be attributed to the emission of the **TCF** conjugated arms. The peak in the longer wavelength region is consistent with the emission peak upon excitation at 519 nm, which proves the energy transfer process in these *meta*-conjugated D-π-A molecules (see Figure S4 in Supporting Information). Moreover, the energy transfer from the **TPA** segments to **TCF** were observed in very dilute solutions (10^{-7} M), which means that this is an intramolecular energy transfer. In the DBA systems with an inert spacer (B), the distinction between Coulombic (Forster) and exchange (Dexter) interactions is quite clear.[57] While in DBA systems with π-conjugated bridges, the super exchange process is preferred. Therefore, in the consideration of the previous discussion, the Dexter or super exchange process might exist in this system, which results in the intramolecular energy transfer. However, the PET process and the super exchange process can both exist in a DBA system.[55−57] With the increase of the concentration, the emission intensity of both the **TPA** and **TCF** segments increased at first. When concentration further increased, the quenching happened at the same time. When the concentration increased to 5×10^{-5} M, all the emission totally quenched.

When the solvent changed to polar DMSO, we observed only a single emission peak from very low concentrations (5×10^{-8} M) to high concentrations (5×10^{-5} M). According to the model compound emission spectra, the emission peak can be attributed to the emission of the **TPA** segment. The disappearance of the emission of the **TCF** arms is also observed in model compound **A3T1** in DMSO, which means the disappearance of the emission is due to the very low quantum efficiency of **TCF** in DMSO. This is because the increase of the polarity of the solvent resulted in a lowered band gap and a stronger electron−photon coupling.

For the expanded system, such as **D2A1T2**, only one peak was observed both in cyclohexane and DMSO (Figure S6 in Supporting Information). The disappearance of the emission peak of the **TCF** arms is could be explained as follows: first, the **TCF**-thienylenevinylene arms intrinsically have low

(56) Soler, M.; McCusker, J. K. *J. Am. Chem. Soc.* **2008**, *130*, 4708–4724.
(57) Pettersson, K; Kyrychenko, A; Rö1nnow, E.; Ljungdahl, T.; Martensson, J.; Albinsson, B. *J. Phys. Chem. A* **2006**, *110*, 310–318.

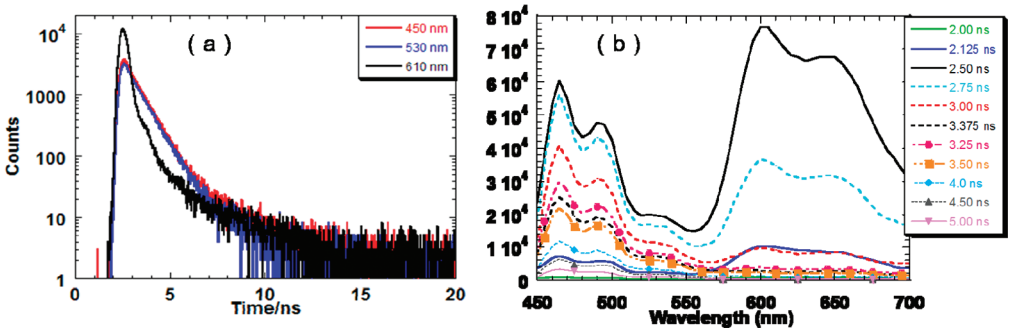

FIGURE 6. (a) Fluorescence decay spectra of **D2A1T1** in cyclohexane collected at different wavelengths. (b) Time-resolved emission spectra of **D2A1T1** excited by 440 nm laser light.

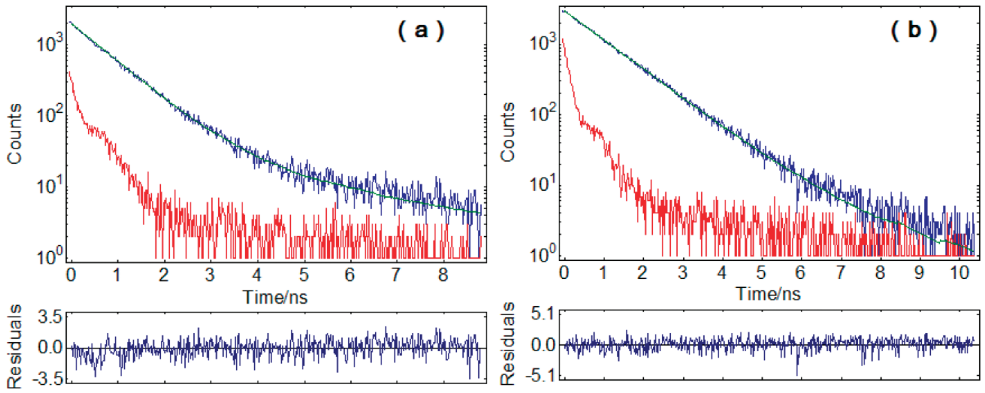

FIGURE 7. Fluorescence decay spectra of **D2A1T1** (left) and **D2A1T2** (right) in cyclohexane.

quantum efficiencies,[58] and second, after introducing the thienylenevinylene, the bandgap of the arms becomes smaller, which would further lower the quantum efficiency.

To gain further insight into the photophysical behavior of these compounds, we investigated the fluorescence lifetime and time-resolved emission spectra of the compounds and reference models in cyclohexane solutions using a time-correlated photon counting instrument (as shown in Figure 6). In Figure 6a, fluorescence decaying spectra of **D2A1T1** collected at 610 nm exhibited a faster decaying speed than those collected at 450 and 530 nm. In Figure 6b, the fluorescence spectra of **D2A1T1** in cyclohexane showed two fluorescence peaks located at around 470 and 600 nm if excited at 440 nm using laser light, and the latter peak was the result of energy transfer. As shown in the figure, no shift of the fluorescence band was observed, while the intensity changed with time. At the beginning (2.00 ns) there were no emission peaks; then the intensity of both peaks gradually increased simultaneously, reached the maximum at 2.50 ns, and finally decreased gradually to zero at 5.00 ns. It is noteworthy that the emission peak of **TCF** segments decreased a bit faster than **TPA** segments, which is consistent with the fluorescence decaying spectra of **D2A1T1**. Both of the peaks appeared at the same time, which indicated the energy transfer process was very fast. Therefore, a super exchange process was preferred in these D-π-A compounds.

The fluorescence lifetimes of these compounds were measured at the concentration of 1×10^{-6} M in cyclohexane. All of these D-π-A compounds exhibited biexponential fluorescence decay, which was indicative of the presence of another fluorescence process in addition to their own fluorescence decaying, whereas the control compounds **D3T1** and **D3T2** can be fit to a single exponential fluorescence decay process (Figure 7). Compounds with different ratios of **TPA** and **TCF** exhibited similar decaying phenomenon and lifetimes. For **D2A1T2**, **D1A1T2**, and **D1A2T2**, a biexponential decaying process of their lifetime was fit a bit longer than that of **D2A1T1**, **D1A1T1**, and **D1A2T1**. The biexponential decaying process indicated that the fluorescence counted at any point in time was reduced by both their own usual radiative decay and intramolecular energy transfer. All time-resolved fluorescence data are presented in Table 3.

TABLE 3. Summary of Fluorescence Lifetimes

compound	τ_1 (ns)	τ_2 (ns)	χ^2
D3T1	0.77		1.12
D2A1T1	0.70	1.70	1.07
D1A1T1	0.55	0.96	1.12
D1A2T1	0.71	3.68	1.18
D3T2	1.08		1.25
D2A1T2	1.03	0.41	1.10
D1A1T2	1.15	0.73	1.12
D1A2T2	1.33	0.54	1.18

Electrochemical Properties. To determine the electrochemical properties and of these compounds and thus to estimate the energy levels of their highest occupied molecular orbital (HOMO) and lowest unoccupied molecular orbital (LUMO), cyclic voltammetry (CV) experiments were performed in THF solutions containing 0.1 M n-Bu_4NPF_6 in

(58) Wang, H.; Lu, Z.; Lord, S. J.; Willets, K. A.; Bertke, J. A.; Bunge, S. D.; Moerner, W. E.; Twieg, R. J. *Tetrahedron* **2007**, *63*, 103–114.

TABLE 4. Summary of Electrochemical Properties

	experimental				calculated[e]		
compound	band gap[a] (eV)	HOMO[b] (eV)	LUMO[c] (eV)	band gap[d] (eV)	HOMO (eV)	LUMO (eV)	band gap (eV)
D2A1T1	1.72	−5.55	−4.25	1.30	−4.76	−3.29	1.47
D1A1T1	1.72	−5.55	−4.25	1.30	−4.82	−3.32	1.50
D1A2T1	1.72	−5.55	−4.25	1.30	−4.87	−3.43	1.44
D2A1T2	1.59	−5.45	−4.35	1.10	−4.65	−3.35	1.31
D1A1T2	1.59	−5.45	−4.35	1.10	−4.68	−3.35	1.33
D1A2T2	1.59	−5.45	−4.35	1.10	−4.73	−3.43	1.31

[a]Estimated from the onset of the absorption at the low-energy edge in solid film. [b]$E_{HOMO} = -[4.65\ V + E_{ox(onset)}]$. [c]$E_{LUMO} = -[4.65\ V + E_{rd(onset)}]$. [d]$E_g = E_{LUMO} - E_{HOMO}$. [e]Computational studies were performed with density functional theory (DFT) using B3LYP/6-31G(d)//B3LYP/3-21G* level.

THF using Ag/AgCl as the reference electrode at a scan rate of 50 mV s^{-1}. The cyclic voltammetry of **D2A1T1**, **D1A1T1**, and **D1A2T1** showed one irreversible oxidation wave peak at around 1.05−1.10 V and one irreversible reduction wave peak at around 0.50−0.60 V versus Ag/AgCl (see Figure S7a in Supporting Information). The HOMO levels were estimated by the onset of the oxidation processes ($E_{HOMO} = -E_{ox} - 4.65$ eV), and the LUMO levels were estimated by the onset of the reduction processes ($E_{LUMO} = E_{rd} - 4.65$ eV). For **D2A1T2**, **D1A1T2**, and **D1A2T2**, the cyclic voltammetry showed one reversible oxidation wave peaks at around 0.90−0.95 V and one reversible reduction wave peaks at around 0.42−0.50 V versus Ag/AgCl. The onset of oxidation waves and reduction waves, by comparison of those of **D2A1T1**, **D1A1T1**, and **D1A2T1**, decreased from about 0.90 eV to about 0.80 eV and from about 0.40 V to about 0.30 V due to the conjugation length extending between donors and acceptors (Figure S7b in Supporting Information). The HOMO, LUMO, and E_g of each compound determined or calculated from data are summarized in Table 4. It is noteworthy that the ratio of donor and acceptor has little influence on the electrochemical properties of these compounds, which is easy to clarify by considering the cross-conjugation property of truxene.[48] The observed electrochemical behavior can be further explained by taking into account the orbital structures and energy levels of the HOMO and LUMO studied by computational methods. Cyclic voltammetry (CV) experiments in films were also performed by drop-casting the THF solutions of the compounds on a glassy carbon electrode in an electrolyte of 0.1 M *n*-Bu_4NPF_6 in acetonitrile using Ag/AgCl as the reference electrode, but we failed to get the reduction wave after many trials (see Figure S8 in Supporting Information).

Conclusions

In conclusion, we have developed a new series of well-defined asymmetric star-shaped π-conjugated molecules. By varying the ratio of **TPA** and **TCF**, the length of linkers, the absorption spectra of donor−acceptor star-shaped conjugated molecules can facilely be tuned. With the increase of the ratio between **TCF** and **TPA**, the relative absorption intensity in longer wavelength region also increases. We are currently trying to modify these star-shaped π-conjugated molecules, mostly by introducing other groups into this tritopic skeleton, which will help us to further investigate the structure−property relation of these unique classes of precisely defined D-π-A conjugated molecules. These *meta*-conjugated systems between donor and acceptor might promote the charge separation process and thus contribute immensely to research of solar cells. Preliminary researches indicate a high correlation between structures and device results and more systematic fabrication of photovoltaic devices from these molecules are underway in our laboratory.

Experimental Section

General Methods. Chemicals were purchased and used as received. All reactions were performed under a nitrogen atmosphere unless stated otherwise. THF were distilled from sodium. ^1H and ^{13}C NMR spectra were recorded on a 300 MHz NMR instrument using $CDCl_3$ as solvent unless otherwise noted. Chemical shifts were reported in parts per million (ppm) relative to internal TMS (0 ppm). UV−vis spectra were recorded on a UV−vis Spectrometer. PL spectra were carried out on a Luminescence Spectrometer. MALDI-TOF mass spectra were recorded on a time-of-flight (TOF) mass spectrometer using a 337 nm nitrogen laser with dithranol as matrix. Elemental analyses were carried out on an instrument. Cyclic voltammetry was performed on a workstation; scan rate, 100 mV s^{-1}; working electrode, glassy carbon electrode; auxiliary electrode, Pt wire; reference electrode, Ag/AgCl; supporting electrolyte, *n*-Bu_4NPF_6 (0.1 M, CH_3CN).

General Procedure for the Knoevenagel Condensation Reaction. To a solution of aldehyde and **TCF** in a mixture of anhydrous THF and EtOH was added NH_4OAc at room temperature under nitrogen atmosphere. The mixture was stirred for 4 h at 60 °C. After 4 h, the reaction mixture was extracted with dichloromethane. The combined organic extracts were washed with water and brine and then dried over $MgSO_4$. After the solvent was removed under reduced pressure, the residue was purified by column chromatography to afford the desired compounds.

D1A1T2. ^1H NMR (300 MHz, $CDCl_3$, ppm): 8.36−8.42 (m, 3H), 7.76−7.81 (d, J = 15.9 Hz, 1H), 7.68−7.72 (m, 6H), 7.20−7.44 (m, 15H), 6.99−7.17 (m, 17H, Ar−H), 6.92−6.96 (dd, J = 3.6 Hz, 2H), 6.84−6.89 (d, J = 15.9 Hz, 1H), 6.63−6.68 (d, J = 15.6 Hz, 1H), 2.95−2.97 (m, 6H), 2.15 (m, 6H), 1.78 (s, 6H), 0.85−0.96 (m, 36H), 0.54−0.62 (m, 30H). ^{13}C NMR (75 MHz, $CDCl_3$, ppm): δ 175.5, 172.9, 154.4, 154.3, 151.6, 147.3, 146.3, 145.4, 145.3, 145.1, 143.4, 143.3, 142.4, 141.7, 141.6, 140.9, 140.5, 140.3, 139.7, 139.0, 138.5, 138.0, 137.9, 137.7, 137.0, 132.3, 131.7, 130.8, 130.4, 129.6, 129.2, 129.1, 128.3, 128.1, 127.7, 127.6, 127.5, 127.2, 127.0, 126.7, 126.0, 125.6, 125.4, 125.2, 124.9, 124.5, 124.3, 124.0, 123.8, 123.6, 123.3, 123.1, 123.0, 121.5, 121.4, 121.3, 121.2, 120.0, 119.6, 119.1, 118.9, 112.7, 112.0, 111.3, 110.8, 97.1, 56.5, 55.8, 37.1, 31.4, 29.4, 26.4, 23.9, 22.2, 13.8. MALDI-TOF MS (m/z): calcd for $C_{125}H_{130}N_4OS_6$ 1894.8, found 1894.8. Anal. Calcd for $C_{125}H_{130}N_4OS_6$: C, 79.15; H, 6.91; N, 2.95. Found: C, 78.95; H, 7.15; N, 2.85.

D1A2T2. ^1H NMR (300 MHz, $CDCl_3$, ppm): 8.34−8.41 (m, 3H), 7.76−7.81 (d, J = 15.9 Hz, 2H), 7.68−7.73 (m, 6H), 7.41−7.45 (dd, J = 3.6 Hz, 2H), 7.22−7.39 (m, 15H), 7.03−7.15 (m, 14H, Ar−H), 6.93−6.97 (dd, J = 3.6 Hz, 2H), 6.84−6.89 (d, J = 15.9 Hz, 1H), 6.64−6.69 (d, J = 15.9 Hz, 2H), 2.95−2.98 (m, 6H), 2.15−2.18 (m, 6H), 1.79 (s, 12H), 0.89−0.98 (m, 36H), 0.59−0.63 (m, 30H). ^{13}C NMR (75 MHz, $CDCl_3$, ppm): δ 175.6, 173.0, 154.5, 154.3, 151.6, 147.3, 146.2, 145.5, 145.3,

145.2, 143.3, 142.4, 141.7, 140.8, 140.3, 139.6, 139.1, 138.5, 138.1, 137.8, 137.1, 132.3, 131.8, 130.7, 130.4, 129.2, 129.1, 128.1, 127.5, 127.1, 126.9, 126.6, 124.9, 124.5, 124.0, 123.6, 123.2, 123.1, 121.3, 121.0, 119.6, 119.0, 112.7, 112.0, 111.4, 110.8, 97.2, 97.0, 56.3, 55.8, 37.0, 31.4, 29.4, 26.4, 23.9, 22.2, 13.8. MALDI-TOF MS (*m*/*z*): calcd for $C_{137}H_{137}N_7O_2S_6$ 2103.9, found 2103.9. Anal. Calcd for $C_{137}H_{137}N_7O_2S_6$: C, 78.13; H, 6.56; N, 4.66. Found: C, 77.95; H, 6.63; N, 4.57.

D2A1T2. ^{1}H NMR (300 MHz, $CDCl_3$, ppm): 8.34−8.46 (m, 3H), 7.76−7.81 (d, J = 15.6 Hz, 1H), 7.68−7.70 (m, 6H), 7.22−7.44 (m, 19H), 6.99−7.14 (m, 24H, Ar−H), 6.92−6.96 (d, J = 3.6 Hz, 4H), 6.84−6.89 (d, J = 15.9 Hz, 2H), 6.62−6.67 (d, J = 15.6 Hz, 2H), 2.97−3.00 (m, 6H), 2.13−2.15 (m, 6H), 1.78 (s, 6H), 0.86−0.94 (m, 36H), 0.59−0.63 (m, 30H). ^{13}C NMR (75 MHz, $CDCl_3$, ppm): δ 175.5, 172.8, 154.5, 154.4, 154.3, 151.6, 147.3, 146.2, 145.4, 145.2, 145.1, 143.4, 142.4, 141.7, 140.9, 140.5, 140.3, 139.7, 139.0, 138.5, 138.0, 137.9, 137.7, 137.0, 132.3, 131.7, 130.8, 130.4, 129.5, 129.2, 129.1, 128.1, 127.5, 127.4, 127.1, 126.6, 124.9, 124.5, 124.3, 124.0, 123.8, 123.6, 123.2, 123.1, 121.4, 120.0, 119.6, 118.9, 112.6, 112.0, 111.3, 110.8, 97.1, 56.4, 55.7, 37.0, 31.4, 29.4, 26.4, 23.9, 22.2, 13.8. MALDI-TOF MS (*m*/*z*): calcd for $C_{145}H_{145}N_5OS_6$: 2163.9, found 2163.9. Anal. Calcd for $C_{145}H_{145}N_5OS_6$: C, 80.40; H, 6.75; N, 3.23. Found: C, 80.16; H, 7.07; N, 3.13.

D1A1T1. ^{1}H NMR (300 MHz, $CDCl_3$, ppm): 8.34−8.46 (m, 3H), 7.83−7.88 (d, J = 15.9 Hz, 1H), 7.75−7.78 (m, 2H), 7.70−7.75 (m, 4H), 7.54−7.58 (m, 2H), 7.48−7.49 (d, J = 3.6 Hz, 1H), 7.37−7.40 (m, 3H), 7.34−7.36 (d, 1H), 7.28−7.31 (m, 3H), 7.12−7.18 (m, 7H), 7.03−7.08 (m, 5H, Ar−H), 6.92−6.98 (d, J = 15.9 Hz, 1H), 6.74−6.80 (d, J = 15.6 Hz, 1H), 2.95−2.97 (m, 6H), 2.15 (m, 6H), 1.82 (s, 6H), 0.85−0.96 (m, 36H), 0.54−0.62 (m, 30H). ^{13}C NMR (75 MHz, $CDCl_3$, ppm): δ 175.6, 173.2, 154.9, 154.3, 154.2, 153.9, 147.4, 147.3, 146.0, 145.5, 145.2, 144.7, 142.7, 142.6, 142.3, 139.6, 139.4, 139.4,139.3, 138.7, 138.3, 138.1, 137.4, 137.2,132.7, 132.6, 140.0, 130.6, 129.3, 128.1, 127.8, 127.1, 127.0, 125.1, 125.0, 124.8, 124.7, 124.7, 124.5, 124.2, 123.8, 123.5, 123.4, 123.1, 123.0, 120.2, 119.7, 118.9, 112.6, 112.0, 111.3, 110.7, 97.4, 97.2, 56.7, 55.8, 37.0, 31.4, 29.4, 26.5, 23.9, 22.2, 13.9. MALDI-TOF MS (*m*/*z*): calcd for $C_{107}H_{118}N_4OS_3$ 1570.85, found 1570.0. Anal. Calcd for $C_{107}H_{118}N_4OS_3$: C, 81.74; H, 7.56; N, 3.56. Found: C, 81.38; H, 7.89; N, 3.38.

D1A2T1. ^{1}H NMR (300 MHz, $CDCl_3$, ppm): 8.35−8.44 (m, 3H), 7.80−7.87 (d, J = 15.9 Hz, 2H), 7.75−7.77 (m, 4H), 7.69−7.71 (m, 2H), 7.55−7.57 (m, 4H), 7.37−7.39 (m, 2H), 7.34−7.36 (d, 1H), 7.28−7.30 (m, 3H), 7.12−7.18 (m, 6H), 7.03−7.07 (m, 5H, Ar−H), 6.92−6.98 (d, J = 15.9 Hz, 1H), 6.76−6.81 (d, J = 15.6 Hz, 2H), 2.95−2.97 (m, 6H), 2.15 (m, 6H), 1.82 (s, 12H), 0.85−0.96 (m, 36H), 0.54−0.62 (m, 30H). ^{13}C NMR (75 MHz, $CDCl_3$, ppm): δ 175.6, 175.3, 173.6, 154.5, 154.0, 153.5, 147.1, 146.1, 145.8, 145.7, 145.5, 142.4, 141.6, 139.8, 139.6, 138.9, 138.7, 138.2, 137.4, 132.5, 130.7, 129.1, 128.8, 127.6, 126.9, 126.8, 125.5, 125.2, 124.9, 124.7, 124.3, 123.7, 123.5, 123.1, 122.9, 122.7, 120.0, 119.9, 119.5, 118.7, 112.5, 112.0, 111.4, 111.0, 110.6, 110.5, 108.9, 104.3, 100.0, 97.4, 97.1, 57.7, 55.7, 36.8, 31.2, 29.1, 26.2, 24.0, 22.0, 13.7. MALDI-TOF MS (*m*/*z*): calcd for $C_{119}H_{125}N_7O_2S_3$ 1779.9, found 1779.0. Anal. Calcd for $C_{119}H_{125}N_7O_2S_3$: C, 80.23; H, 7.07; N, 5.50. Found: C, 79.85; H, 7.18; N, 5.18.

D2A1T1. ^{1}H NMR (300 MHz, $CDCl_3$, ppm): 8.34−8.46 (m, 3H), 7.83−7.88 (d, J = 15.6 Hz, 1H), 7.75−7.79 (m, 2H), 7.69−7.72 (m, 4H), 7.55−7.57 (m, 2H), 7.37−7.39 (d, J = 3.6 Hz, 4H), 7.28−7.31 (m, 9H), 7.12−7.18 (m, 11H), 7.03−7.08 (m, 10H, Ar−H), 6.92−6.97 (d, J = 15.9 Hz, 2H), 6.75−6.80 (d, J = 15.6 Hz, 1H), 2.95−2.97 (m, 6H), 2.15 (m, 6H), 1.82 (s, 6H), 0.85−0.96 (m, 36H), 0.54−0.62 (m, 30H). ^{13}C NMR (75 MHz, $CDCl_3$, ppm): δ 175.6, 175.3, 173.6, 154.5, 153.9, 153.5, 147.1, 146.1, 145.8, 145.7, 145.5, 142.4, 141.6, 139.8, 139.6, 138.9, 138.7, 138.2, 137.4, 132.5, 130.7, 129.1, 128.8, 127.6, 126.9, 126.8, 125.5, 125.2, 124.9, 124.7, 124.3, 123.7, 123.5, 123.1, 122.9, 122.7, 120.0, 119.95, 119.86, 119.5, 118.7, 112.5, 112.0, 111.4, 111.0, 110.6, 110.4, 108.9, 104.3, 99.9, 97.4, 97.1, 57.7, 55.7, 36.8, 31.2, 29.1, 26.2, 24.0, 22.0, 13.7. MALDI-TOF MS (*m*/*z*): calcd for $C_{127}H_{133}N_5OS_3$ 1839.9, found 1839.0. Anal. Calcd for $C_{127}H_{133}N_5OS_3$: C, 82.83; H, 7.28; N, 3.80. Found: C, 82.47; H, 7.63; N, 3.39.

Acknowledgment. This work was supported by the Major State Basic Research Development Program (Nos. 2006CB921602 and 2009CB623601) from the Ministry of Science and Technology and the National Science Foundation of China.

Supporting Information Available: Experimental procedures, ^{1}H and ^{13}C NMR, and elemental analysis of all new compounds. Theoretical calculated absolute energies and tables of atom coordinates. This material is available free of charge via the Internet at http://pubs.acs.org.